Spectroscopic Studies of Dual Fluorescence in 2-((4-Fluorophenyl)amino)-5-(2,4-dihydroxybenzeno)-1,3,4-thiadiazole

ARTICLE *in* THE JOURNAL OF PHYSICAL CHEMISTRY A · OCTOBER 2015

Impact Factor: 2.69 · DOI: 10.1021/acs.jpca.5b06475

7 AUTHORS, INCLUDING:

Arkadiusz Matwijczuk

University of Life Sciences in Lublin

26 PUBLICATIONS **45** CITATIONS

SEE PROFILE

Andrzej Górecki

Jagiellonian University

24 PUBLICATIONS **170** CITATIONS

SEE PROFILE

Agnieszka Ludwiczuk

Medical University of Lublin

51 PUBLICATIONS **326** CITATIONS

SEE PROFILE

THE JOURNAL OF PHYSICAL CHEMISTRY A

Article

pubs.acs.org/JPCA

Spectroscopic Studies of Dual Fluorescence in 2-((4-Fluorophenyl)amino)-5-(2,4-dihydroxybenzeno)-1,3,4-thiadiazole

Arkadiusz Matwijczuk,*[,†] Daniel Kamiński,[‡] Andrzej Górecki,[§] Agnieszka Ludwiczuk,[∥] Andrzej Niewiadomy,[‡] Sebastian Maćkowski,[⊥] and Mariusz Gagoś*[,#]

[†]Department of Biophysics and [‡]Poland Department of Chemistry, University of Life Sciences in Lublin, 20-950 Lublin, Poland

[§]Department of Physical Biochemistry, Faculty of Biochemistry, Biophysics and Biotechnology of the Jagiellonian University, 31-007 Kraków, Poland

[∥]Chair and Department of Pharmacognosy with Medicinal Plant Unit, Medical University of Lublin, 1 Chodzki Str., 20-093 Lublin, Poland

[⊥]Institute of Physics, Faculty of Physics, Astronomy and Informatics, Nicolaus Copernicus University, 87-100 Toruń, Poland

[#]Department of Cell Biology, Institute of Biology, Maria Curie-Skłodowska University, 20-033 Lublin, Poland

Supporting Information

ABSTRACT: The paper presents results of fluorescence analysis of ionic and nonionic 2-((4-fluorophenyl)amino)-5-(2,4-dihydroxybenzeno)-1,3,4-thiadiazole (FABT) in monocrystals and solutions. We found a single fluorescence band in the case of FABT crystals grown in methanol and dual fluorescence for FABT crystals grown in an aqueous environment. The effect of dual fluorescence was preserved for FABT dissolved in aqueous solutions with pH ranging from 7.5 to 1. In contrast, FABT dissolved in methanol exhibited a single fluorescence band. The dual fluorescence effect is associated with conformational changes in the FABT molecule, which can be induced by aggregation effects. On the basis of crystallographic data, two types of FABT crystal molecule conformations were distinguished. In methanol, FABT molecules are in conformation "S" (the −OH group from the resorcyl ring oriented toward the sulfur atom from the 1,3,4-thiadiazole ring), which a gives single fluorescence band. In water, FABT in conformation "N" (the −OH group from the resorcyl ring oriented toward the nitrogen atom from the 1,3,4-thiadiazole ring due to 180° rotation) has two fluorescence bands. This significant finding implies the possibility of performing a rapid analysis of conformational changes in FABT molecules using fluorescence spectroscopy both in solutions and in biological samples.

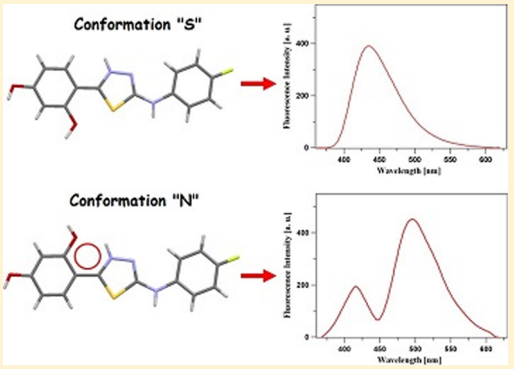

INTRODUCTION

1,3,4-Thiadiazoles with a substituted resorcyl fragment are one of the most effective and promising agents in fighting many diseases, especially those with a neoplastic background. In general, thiadiazoles are five-membered ring systems containing two nitrogen atoms and one sulfur atom. The first 1,3,4-thiadiazole was described by Fischer in 1882, but the actual nature of these ring systems was presented in 1890 by Freund and Kuh.[1,2] The activity of 1,3,4-thiadiazoles is based on the presence of a thioimine group incorporated into the cyclic system in their structure, which can be regarded as a rigid analogue of the tautomeric form of the thioamide bond. All representatives of this group of compounds containing the ring system mentioned above have been widely applied in medicine as oxidation inhibitors, cyan dyes, or metal complexing compounds.[3−6] The literature describes the entire family of thiadiazoles as compounds with, e.g., anticancer,[7] antifungal,[8] antibacterial, anticonvulsant,[9] diuretic, anti-inflammatory,[10] antiviral, antituberculotic, antihypertensive, antidepressant, or antioxidative[11] activities. Despite their importance in biology and medicine, the mechanism of their action is still poorly known. To better understand the mechanisms underlying their biological activity, we investigated molecular interactions of 2-((4-fluorophenyl)amino)-5-(2,4-dihydroxybenzeno)-1,3,4-thiadiazole (FABT, Scheme 1A)[10,12−14] with different solvents.

The aim of the present study was to perform spectroscopic analyses of the molecular organization of FABT in organic solvents and in an aqueous environment at different concentrations of hydrogen ions. Using spectroscopic methods based on electronic absorption spectroscopy, fluorescence, and resonance light scattering (RLS) techniques, the complexity of the physical processes responsible for the phenomenon of dual fluorescence in FABT was elucidated. With the use of fluorescence spectroscopy supported by X-ray crystallography, we coherently describe the phenomenon of dual fluorescence of FABT molecules in an aqueous environment. Crystallographic

Received: July 6, 2015
Revised: October 14, 2015

DOI: 10.1021/acs.jpca.5b06475
J. Phys. Chem. A XXXX, XXX, XXX−XXX

Scheme 1. Chemical Structure of the FABT Molecule (A, Enol Form; B, Form Ionized with the $-O^-$ Group; C, Form Ionized with the $-N^+-H$ Group, in Which the −OH Group Is Located on the Side of the N−H Group from the 1,3,4-Thiadiazole Ring; D, Form Ionized with the $-N^+-H$ Group, in Which the −OH Group Is Located on the Side of Sulfur from the 1,3,4-Thiadiazole ring)

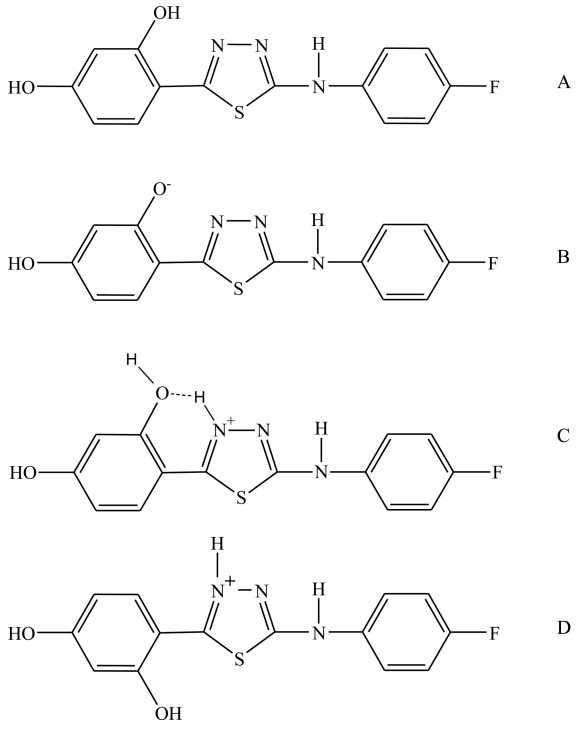

studies indicate possible rotation of the resorcyl fragment of the molecule depending on the crystal solvates as the source of this effect.

The dual fluorescence effect is related to the appearance of two clearly distinct emission bands upon light excitation.[15−20] The effect is induced by solvent polarity, environmental pH, and temperature. One of the main explanations of the dual fluorescence effect is the appearance of intramolecular CT states[21,22] with twisted intramolecular charge transfer states (TICT).[23−25] A textbook example of a molecule with the TICT state is the (*N*,*N*-dimethylamino)benzonitrile molecule (DMABN). The TICT model introduced in the seventies[26] by K. Rotkiewicz, K. H. Grellmann, and Z. R. Grabowski, despite their different views on its mechanism, has become one of the best-known models in experimental[27] and theoretical[28] investigations in photophysics and molecular spectroscopy. Another equally interesting and highly popular approach in explaining the dual fluorescence phenomenon is the excited-state intramolecular proton transfer called ESIPT.[25,29−37] This effect was observed for organic molecules, in which the acceptor group is located in close proximity to the proton donor group. These processes of intramolecular proton transfer by excitation states have been a focus of many experimental and theoretical investigations as well.[38−43]

We applied fluorescence spectroscopy to study the influence of the molecular organization of the FABT in solvents and an aqueous environment on the dual fluorescence effect and its dependence on the hydrogen ion concentration, temperature, polarity of the solvent, and aggregation.

Knowledge of the details of the organization of the FABT molecules in an aqueous environment and other organic solvents may help to understand 1,3,4-thiadiazole protein interactions in biological systems. Recently, thiadiazoles attract scientific interest because of they properties: HSP90 inhibitor, glycolate oxidaze inhibitor, carbonic anhydraze II inhibitor and other protein complexes.[44−47] Fast spectroscopic characterization of thiadiazole N,S-conformation in protein pockets compared to protein crystallography and NMR can facilitate investigation of such interaction.

MATERIAL AND METHODS

Materials. The 2-(4-fluorophenylamino)-5-(2,4-dihydroxybenzeno)-1,3,4-thiadiazole (FABT) (Scheme 1A) was synthesized in the Department of Chemistry of the University of Life Sciences in Lublin; details of the procedure are described elsewhere.[10] The structure of the FABT is presented in the Cambridge Crystallographic Data Centre with entries: CCDC 768785−768787.

The purification procedure of the FABT compound is described in detail in refs 48 and 49.

All solid phase measurements of FABT were carried out on crystals obtained from a mixture of alcohol, such as methanol, propan-2-ol, or butanol, and 2 M HCl as a protonating agent (4:1 v/v). Suitable crystals were grown at room temperature for 3 weeks. The alcohol to water ratio in the crystallization mixture (during alcohol evaporation) was 1:1. A lower concentration of alcohol led to formation of alcohol-free crystals. Moreover, a small amount of characteristic dark yellow alcohol-free FABT crystals was grown in the aqueous solution. The alcohol (e.g., propan-2-ol) containing crystals were light yellow. The crystals grown from the mixture of butanol/water did not contain alcohol and even at the ratio 6:1 only crystalline hydrates were present. The more detailed protocols for crystallization of FABT together with the characterization of crystals obtained were reported in our previous work.[48,49] The crystallographic structures are presented in the Supporting Information.

Methods. All solutions were measured with an Elmetron CP-502 pH-meter at room temperature. For FABT−methanol solutions, FABT was first dissolved in methanol and then the pH was changed by slow addition of 0.1 M HCl to the glass flask. For water−FABT solutions, 0.1 M NaOH was added first to water to obtain pH 12. Afterward, powder FABT was dissolved in it. To obtain a certain pH of the water−FABT solution, 0.1 M HCl acid was slowly added. The pH was continually controlled. Electronic absorption spectra of FABT were recorded on a double-beam UV−vis spectrophotometer Cary 300 Bio (Varian) equipped with a thermostated cuvette holder with a 6 × 6 multicell Peltier block. Temperature was controlled with a thermocouple probe (Cary Series II from Varian) placed directly in the sample.

Fluorescence excitation, emission, and synchronous spectra were recorded with a Cary Eclipse spectrofluorometer (Varian) at 22 °C. Fluorescence spectra were recorded with 0.5 nm resolution and corrected for the lamp and photomultiplier spectral characteristics. Resonance light scattering (RLS) measurements were performed as in Pasternack and Collings.[50] The excitation and emission monochromators of the spectrofluorometer were scanned synchronously (0.0 nm interval between excitation and emission wavelengths); the slits were set to obtain spectral resolution of 1.5 nm. The

DOI: 10.1021/acs.jpca.5b06475
J. Phys. Chem. A XXXX, XXX, XXX−XXX

spectral analysis was performed with the use of Grams/AI 8.0 software (Thermo Electron Corporation).

Raman scattering spectra of the liquid samples placed onto a quartz plate were recorded with the inVia Reflex Raman Microscope from Renishaw equipped with two holographic ultrahigh precision diffraction grating stages and a high sensitivity ultralow noise CCD detector (RenCAM). A 785 nm Ar^+ ion laser was used to record Raman scattering. The spectra were accumulated within a 10 s integration time. All experiments were carried out at 22 °C. Spectral analysis was performed with Grams/AI 8.0 software (Thermo Electron Corporation).

Time-correlated single photon counting (TCSPC) measurements were performed on a FluoroCube fluorometer (Horiba, France). The samples were excited with pulsed NanoLED diode at 372 nm (pulse duration of 150 ps) operated with 1 MHz repetition. To avoid pulse pile-up, the power of the pulses was adjusted to an appropriate level using a neutral gradient filter. Fluorescence emission was recorded using a picosecond detector TBX-04 (IBH, JobinYvon). The DataStation and the DAS6 software (JobinYvon (IBH)) were used for data acquisition and signal analysis. All fluorescence decays were measured in a 10 × 10 mm quartz cuvette, using an emitter cutoff filter with transmittance for wavelengths longer than 408 nm. The excitation profiles required for the deconvolution analysis were measured without the emitter filters on a light scattering cuvette. All measurements were performed in water either at 20 °C and various pH or at pH 7 and increasing (or decreasing) temperature. Each fluorescence decay was analyzed with a multiexponential model given by the equation:

$$I_t = \sum_i \alpha_i \exp(-t/\tau_i) \quad (1)$$

where α_i and τ_i are the pre-exponential factor and the decay time of component i, respectively.

Best-fit parameters were obtained by minimization of the reduced χ^2 value as well as residual distribution of experimental data. The average lifetime of fluorescence decay was calculated according to the following equation:

$$\langle \tau \rangle = \frac{\sum_i \alpha_i \tau_i^2}{\sum_i \alpha_i \tau_i} \quad (2)$$

CD measurements were carried out on a J-815 circular dichroism spectrometer (JASCO) using a quartz cell of 1 cm path length. Spectra were recorded at 21 °C from 240 to 500 at 0.2 nm resolution with a scan rate of 20 nm/min. Raw data were manipulated by smoothing.

RESULTS AND DISCUSSION

The crystallographic analyses have shown that, due to solvatomorphism, the nonionic FABT and ionic $FABTH^+$ (crystals grown at pH = 1) forms of the molecule can have two types of conformation: the "S" conformation (Scheme 1D, the −OH group from the resorcyl ring oriented toward the sulfur atom from the 1,3,4-thiadiazole ring) and the "N" conformation (Scheme 1C, the −OH group from the resorcyl ring oriented toward the nitrogen atom from the 1,3,4-thiadiazole ring due to 180° rotation).[49] With the DFT methods, the difference in energy between the two conformers ("N" and "S") was estimated at 3.2 kcal/mol; in turn, the rotating barrier for the analyzed molecule was calculated to be 12.6 kcal/mol.[49] On the basis of potentiometric FABT titration, we determined characteristic pK points for the ionization-related −OH groups in the resorcyl ring and for the $-N^+-H$ group in the 1,3,4-thiadiazole ring, Scheme 1. pK = 8.6 for the −OH group in the *ortho* position in the resorcyl ring and pK = 4.3 for the $-N^+-H$ group were found. Therefore, it can be assumed that in physiological conditions a majority of FABT molecules are ionized and adopt forms presented in Scheme 1C and D.[49]

To explore the character of molecular interactions in the crystals (from which the FABT/$FABTH^+$ structures were determined), fluorescence spectra of the solvates were analyzed. Panel A in Figure 1 presents fluorescence emission spectra of

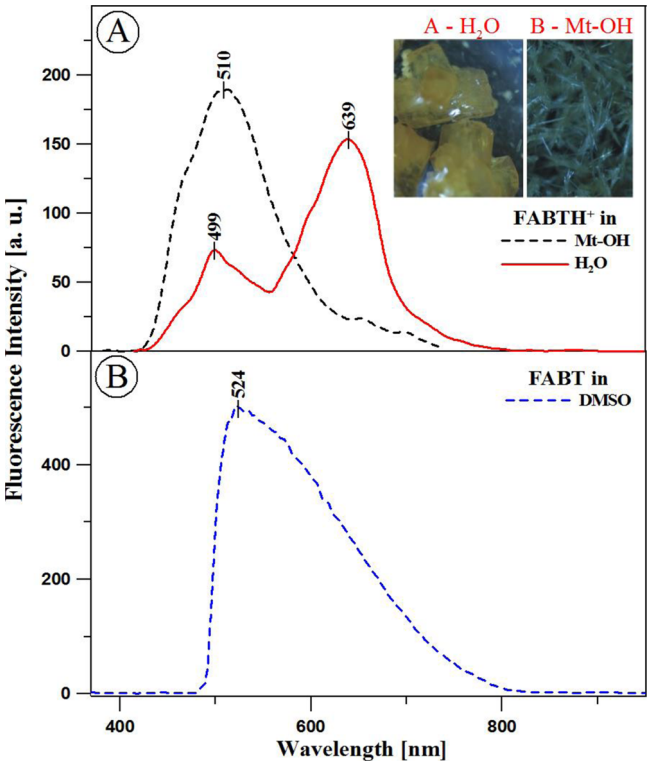

Figure 1. Panel A: fluorescence emission spectra of crystals of the ionic FABT forms (obtained at pH 1) grown in H_2O (red line) and methanol (dotted black line). The excitation wavelength for both crystals was 340 nm. The inset presents microscopic images of the FABT monocrystals obtained in water (A) and methanol (B). Panel B: fluorescence emission spectra of FABT crystals growing in DMSO (dotted blue line). The excitation wavelength was 340 nm.

$FABTH^+$ monocrystals (excitation at 340 nm): H_2O solvate (red line) and methanol solvate (dashed black line). In the case of the $FABTH^+$ emission spectrum of the H_2O solvate, dual emission was observed with a maximum at 499 and 639 nm. In turn, single fluorescence with a maximum at 510 nm was visible in the case of the $FABTH^+$ methanol solvate. The crystallographic analysis showed that the $FABTH^+$ molecule in methanol adopted the "S" conformation (single fluorescence), whereas the $FABTH^+$ in H_2O exhibited the "N" conformation (dual fluorescence), as shown in Scheme 1C,D, respectively.[49]

To compare the spectroscopic properties of FABT crystals, we performed analogous measurements of fluorescence emission spectra of crystals in a nonionic form obtained in DMSO (Figure 1, panel B). The excitation wavelength was 340 nm. Crystallographic analysis revealed that the FABT molecule whose crystals grew in DMSO had a structure presented in

DOI: 10.1021/acs.jpca.5b06475
J. Phys. Chem. A XXXX, XXX, XXX−XXX

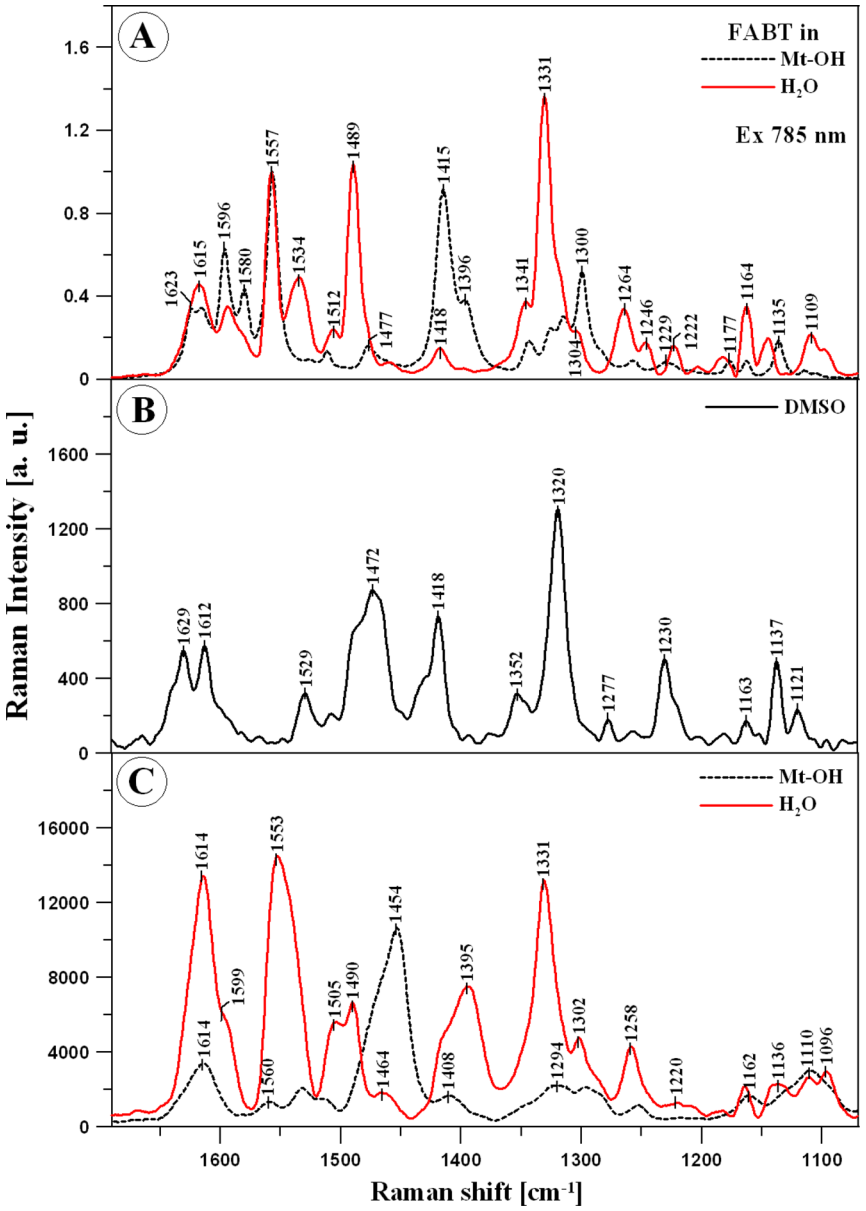

Figure 2. Panel A: Raman spectra of the monocrystals of the ionic FABT forms obtained in water (red line) and in methanol (dotted black line). Panel B: Raman spectra of the monocrystals of the nonionic FABT forms obtained in DMSO (solid black line). The measurements were performed at excitation radiation with a wavelength of 785 nm at a temperature of 22 °C. Panel C: Raman spectra of FABT obtained in the aqueous solution at pH 1 (red line) and in methanol (dotted black line). The measurements were performed at excitation radiation with a wavelength of 785 nm at a temperature of 22 °C.

Scheme 1A, where the −OH group is oriented toward the nitrogen atom in the thiadiazole ring. In this case, single rather than dual fluorescence with a maximum at 524 nm and greatly widened in comparison to the emission spectrum of the $FABTH^+$ Mt−OH solvate can be observed, Figure 1.

Application of Raman Spectroscopy in the Analysis of $FABTH^+$ Monocrystals. Considerable spectral changes in the two forms of $FABTH^+$ monocrystals can be observed in the Raman spectra. Figure 2, panel A, presents Raman spectra intensity normalized at the frequency of 1557 cm^{-1} for $FABTH^+$ in the H_2O solvate (red line) and the methanol solvate (dashed black line). The samples were excited at 785 nm at 22 °C. To facilitate further discussion, positions of the major $FABTH^+$ Raman bands are listed in Table 1. For comparison, the Supporting Information includes Gaussian09 calculations for Raman spectra. As revealed by the comparison of the Raman spectra of $FABTH^+$ composed of the methanol solvate ("S" conformation) with the Raman spectra of the $FABTH^+$ H_2O solvate ("N" conformation), new bands appear with maxima at 1534, 1489, 1331, 1264, 1164, and 1109 cm^{-1}. These bands are characteristic for stretching vibrations of the C═C, C═N, C—C, and deformation vibration of C—H groups in the $FABTH^+$ molecule.

The aforementioned change in the position of the −OH group from the resorcyl ring (in the *ortho* position) in relation to the 1,3,4-thiadiazole system exerts an impact on the spectral changes observed in the $FABTH^+$ Raman spectra. The geometry of the system (Scheme 1C) facilitates formation of a so-called *pseudo heteroaromatic* ring, which is responsible for the new bands observed in Raman spectroscopy. The bands are

DOI: 10.1021/acs.jpca.5b06475
J. Phys. Chem. A XXXX, XXX, XXX−XXX

Table 1. Position of the Raman Spectral Maxima Together with Assignment of Respective Vibrations to FABT Obtained from Crystals in Methanol and in Water in the 1700−1000 cm^{-1} Spectral Range and for FABT Obtained in Water and Methanol Solutions at pH 1[a]

position of bands (cm^{-1})					
solvents		crystals			
Mt−OH pH 1 (Int)	H_2O pH 1 (Int)	Mt−OH (Int)	H_2O (Int)	DMSO (Int)	type and origin of vibrations
		1623 (28620)		1629 (558)	$\nu(C{-}N)_s$, $\nu_{ring,\ s}$
1614 (3547)	1614 (13439)	1617 (28621)	1617 (9255)	1612 (578)	$\nu_{ring,\ s}$
	1599 (6267)		1593 (7319)		$\nu(N{-}H)_m$, $\nu(C{=}N)_m$, $\nu(C{=}C)_m$
1560 (1519)	1553 (14563)		1557 (21704)		$\nu_{rings,\ vs}$, $\delta(N{-}H)_{vs}$
1536 (2063)		1529 (7995)	1534 (9762)	1529 (324)	$\nu_{rings,\ m}$, $\delta(N{-}H)_m$, ν $(C{=}N)_m$
	1505 (5651)	1512 (11434)	1505 (4920)		$\nu(C{=}C)_w$, $\nu(OH)_w$
	1490 (6627)	1477 (13346)	1489 (22535)	1472 (867)	$\nu_{vs}(C{=}C)$, $\nu_{ring,\ vs}$, $\delta(N{-}H)_s$
1454 (10651)	1464 (1919)	1467 (8070)	1459 (1601)		$\nu(N{-}H)_w$, $\delta(C{-}H)_w$, $\nu(C{=}C)_w$
1408 (1699)	1395 (7607)	1421 (6982)	1418 (2985)	1418 (737)	$\nu_{ring,\ vs}$, $\delta(N{-}H)_{vs}$, $\delta(C{-}H)_s$
			1346 (7595)	1352 (328)	$\nu(C{=}C)_m$, $\delta(N{-}H)_w$, $\nu_{ring,\ w}$
	1331 (13259)		1330 (29221)	1320 (1304)	$\nu(N{-}H)_{vs}$, $\nu(N{=}N)_{vs}$, $\nu_{ring,\ vs}$
1320 (2279)		1316 (25568)	1304 (4920)		$\nu(N{-}H)_m$, $\nu(N{=}N)_m$, $\nu_{ring,\ w}$
1294 (2099)	1302 (4851)	1298 (43647)	1265 (6813)	1277 (178)	$\nu(N{=}N)_m$, $\nu(N{-}H)_w$
1252 (1155)	1258 (4491)		1247 (3723)		$\nu(N{-}H)_w$, $\nu(C{-}H)_w$
	1220 (1447)	1227 (6982)	1223 (3354)	1230 (514)	$\nu(N{-}H)_w$, $\nu(C{-}H)_w$, $\nu_{ring,\ w}$
			1204 (1187)		$\nu(N{-}H)_w$, $\nu(C{-}H)_w$, $\nu_{ring,\ w}$
1162 (1735)			1183 (2108)	1163 (1163)	$\delta(C{-}C)_m$, $\nu(N{=}N)_m$, $\nu(C{-}H)_m$
1131 (2027)	1136 (2315)	1165 (7489)	1162 (8009)	1137 (483)	$\delta(C{-}H)_w$
		1107 (3543)	1144 (4367)	1121 (229)	$\nu(N{=}N)_w$, $\nu(C{-}H)_w$
1110 (3079)			1109 (4553)	1151 (114)	$\nu(N{=}N)_w$, $\nu(C{-}H)_w$
	1096 (2967)	1063(7680)	1097 (2939)		ν_{ring}, $\delta(C{-}H)$

[a]The asterisk (*) indicates vibrations that may originate from the solvents tested. Key: ν = stretching vibrations, δ = deformation vibrations, s = symmetric, as = asymmetric, vs = very strong, s = strong, m = medium, w = weak, vw = very weak. Int = intensity of vibration (au).

not observed for the "S" conformation like in $FABTH^+$ H_2O (Scheme 1D). The "N" type of conformation may be associated with the intramolecular charge transfer in the $FABTH^+$ molecule, which may be related to the observed phenomenon of dual fluorescence. Because the $FABTH^+$ crystalline structures described above were solvates of the analyzed molecule, the subsequent stage of the investigation of the molecular mechanisms of crystal growth involved acquisition of the nonionic FABT form, which proved highly useful in elucidating mechanisms of the keto/enol equilibrium[14] and the dual fluorescence effect in water observed for the FABT molecule. The monocrystal was grown from FABT dissolved in DMSO.[49] The nonionic structure obtained is primarily stabilized by hydrogen bonding interactions between FABT and DMSO molecules as well as a network of hydrogen bonds between adjacent FABT molecules. During FABT crystal growth in DMSO, a possibility of emergence of two polymorphic forms of the analyzed molecule was also observed.[48]

The position of the −OH group (Scheme 1C,D) from the resorcyl ring (in the *ortho* position) seems to be the most important information for further discussion. The −OH group is located at the nitrogen atom of the 1,3,4-thiadiazole ring ("N" conformation). For the ionic crystalline forms obtained in water, the −OH group was located in the same position. In contrast, in the methanol solvate, the group was rotated by ∼180° with respect to the rest of the molecule. The quantum-mechanical calculations show that the "N" conformation is energetically more preferable for a single molecule.[49] For this reason, the "N" conformation is dominant in the aqueous solution. Furthermore, a hydrogen bond may be formed between the aforementioned groups. This molecule conformation in the solution of *n*-heptane and similar solvents may facilitate proton transfer and formation of a keto form of the FABT molecule.[14]

To confirm the considerations presented above, the Raman spectrum of the crystalline FABT form in DMSO was measured in the subsequent stage of the analysis of the molecular mechanisms. Figure 2 (panel B) presents a Raman FABT spectrum of a monocrystal in the range 1050−1700 cm^{-1}. To facilitate discussion, Table 1 shows the location of the main Raman bands for the spectrum obtained together with assignment of their functional groups. The measurements were performed as in the case of the ionic forms at an excitation wavelength of 785 nm and at 22 °C. Detailed analysis of the spectrum obtained and comparison thereof with spectra of the crystalline ionic forms described above reveal characteristic intense bands, which rather correspond to bands observed for the ionic $FABTH^+$ form. These bands can be observed in the spectra of the $FABTH^+$ H_2O solvate, but they do not appear in the spectra of the methanol solvate. The band with a maximum at 1529 cm^{-1} corresponds to the stretching vibrations of the C═N group in the 1,3,4-thiadiazole ring in combination with the vibrations of the ring itself. In the case of the FABT monocrystals grown in water, the band at 1534 cm^{-1} is also characteristic for imino NH stretching vibrations. In turn, the band with a maximum at 1472 cm^{-1} corresponds to C═N stretching vibrations and C═C stretching vibrations between the thiadiazole and resorcyl rings; for the $FABTH^+$ H_2O solvate, this band is also underpinned by imino NH stretching vibrations. The next bands with maxima at 1352 and 1320 cm^{-1} were assigned to stretching vibrations of the C═N group in the thiadiazole ring in combination with C═C stretching vibrations in the thiadiazole ring. Other characteristic bands include those at 1230 and 1163 cm^{-1}, which correspond to C—

DOI: 10.1021/acs.jpca.5b06475
J. Phys. Chem. A XXXX, XXX, XXX−XXX

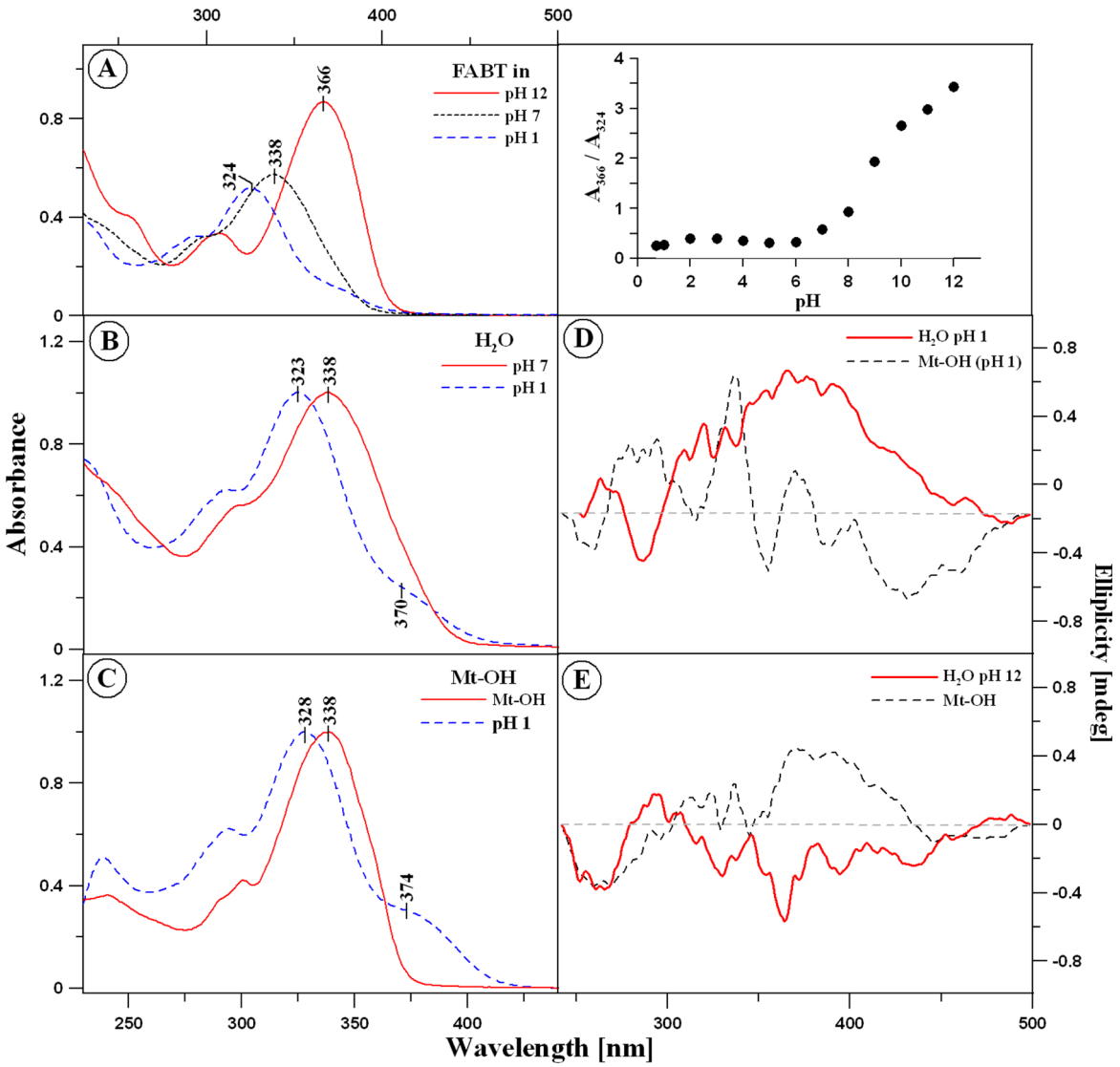

Figure 3. Electron absorption spectra of FABT obtained in the aqueous solution at pH 12, 7, and 1 (panel A). Normalized electron absorption spectra of FABT obtained in the aqueous solution at pH 7 and 1 (red line and dotted blue line, respectively), panel B, and for comparison, in methanol and methanol solution acidified to pH 1, panel C (red line and dotted blue line, respectively). The inset next to panel A presents the ratio of the absorption maximum at 366 to 324 nm depending on changes in the pH of the environment. Panels D and E: CD spectra of FABT (panel D) dissolved in water (pH 1) and methanol (pH 1) and (panel E) dissolved in water (pH 12) and pure methanol.

C stretching vibrations (or imino NH deformation vibrations) and C—C deformation vibrations, respectively. As can be seen, the Raman spectrum obtained from the FABT DMSO solvates is similar to that for the H_2O solvates. It should be emphasized that the dual fluorescence phenomenon was not observed for the FABT crystals grown in DMSO.

The Raman band with a maximum at 1489 cm^{-1} appearing for the H_2O and DMSO solvates seems to be the most important for further elucidation of the dual fluorescence phenomenon. This band completely disappears in the case of the FABTH Mt−OH solvate. It is a result of vibrations of the imino NH group in combination with C═N and C═C stretching vibrations between the 1,3,4-thiadiazole and resorcyl rings.

Spectroscopic Studies of the Dual Fluorescence Effect in Solvents. Analyses of FABT in the aqueous solution performed in the entire range of hydrogen ion concentrations indicate distinct changes, particularly in the region that is important for physiological values. It should be mentioned that, contrary to crystals, in the solution at different pH values, FABT can occur in all forms presented in Scheme 1; therefore, we will hereafter use the FABT abbreviation for all the forms. Figure 3 (panel A) presents electronic absorption spectra of FABT obtained at different pH values (pH 1, 7, and 12, respectively). Dissociation of the −OH group from the resorcyl ring in the *ortho* positon (Scheme 1B) causes a 2264 cm^{-1} hypsochromic shift in the case of the FABT spectrum at pH 12 and a 1278 cm^{-1} bathochromic shift for the spectrum at pH 1 relative to the spectrum at pH 7. Together with the ionization process, aggregation of the compound is possible. The broadening of the FABT absorption spectrum at pH 7 implies the possible presence of other than monomeric spectral forms of the compound.[51] In the case of the FABT spectrum at pH 1, the absorbance of the compound is the lowest, which may suggest dominance of aggregated forms.

The inset in Figure 3 (panel A) presents the ratio of the absorbance maximum at 366 nm (predominant monomeric form) to 324 nm (predominant associated form) depending on

DOI: 10.1021/acs.jpca.5b06475
J. Phys. Chem. A XXXX, XXX, XXX−XXX

the pH value of the aqueous solution. As can be seen, the level of FABT monomerisation (i.e., the predominance of the monomeric form) is the highest at pH 12 and the lowest at pH 1. The greatest changes in the presented ratio are particularly evident at a physiological pH value.

Figure 3 (panels B and C) presents electronic absorption spectra of FABT in the aqueous solution with pH 7 (panel B, red line) and in the same solution acidified with 0.1 M HCl to obtain pH 1 (dashed blue line). For the sake of comparison, both spectra were normalized at a maximum wavelength ~430 nm. Analogically, panel C presents electron absorption spectra of FABT obtained in the same conditions, but the crystals were dissolved in methanol (red line) and methanol acidified to pH 1 (dotted blue line). Clearly, both hypsochromic and bathochromic shifts are concurrently observed in both samples at pH 1. In the case of FABT dissolved in the aqueous solution, there is a splitting of the 338 nm (29 586 cm^{-1}) band, which is observed at pH 7, to two bands at pH 1. The shift to longer wavelengths ("red shift") is observed at 370 nm (27 027 cm^{-1}) and the shift to shorter wavelengths ("blue shift") is observed at 323 nm (30 960 cm^{-1}). The $\Delta\nu$ between 338 and 370 nm is 2559 cm^{-1}. In the case of FABT dissolved in methanol and methanol with pH 1, we can observe a red shift from 338 nm (29 586 cm^{-1}) to 374 nm (26 738 cm^{-1}) with $\Delta\nu$ = 2848 cm^{-1} and a blue shift from 338 to 328 nm (30 488 cm^{-1}). This effect is characteristic and involves processes associated with molecular aggregation.[51−55]

Based on the exciton splitting theory and the spectral shifts, it was possible to calculate the distance between adjacent chromophores of the FABT molecules.[56−58] In the case of the FABT dimers in the aqueous solution, the distance between the adjacent chromophores was calculated at 3.71 Å, whereas that in methanol was 3.97 Å.[52,53] These results are consistent with crystallographic data, which showed a distance of 3.32 Å between the adjacent molecules in H_2O solvate, whereas the distance in the case of methanol solvate was 3.42 Å.[49]

To investigate the potential differences in the conformation of the analyzed molecules and their effect on the dual fluorescence effect, the circular dichroism CD spectra were measured. CD spectroscopy is an excellent tool for investigation of excitonic interactions in aggregated molecular systems. Figure 3 (panel D) presents CD spectra of FABT dissolved in H_2O at pH 1 and in methanol at pH 1 (apparent pH). As can be seen, the CD signal of the sample is very weak. This implies that the aggregated structures formed by the molecules do not exhibit distinct chirality centers or that the transition dipole moments of aggregates (mostly dimers) are almost parallel, similar to the case in crystal structures. Panel E shows corresponding CD spectra of FABT in water and in methanol at pH 12. A clearly different Cotton effect can be noticed for the analyzed samples. A positive Cotton effect is observed in the entire range of the presented spectrum of FABT in H_2O at pH 1; in turn, in methanol (at pH 1), the Cotton effect is negative for wavelengths from 500 to ~350 nm and clearly changes into a positive effect at approximately 350 nm. The change in the value of the pH of the environment is accompanied by spectral changes, which proves conformational changes in the analyzed molecules. For FABT in water at pH 12, we observe a slight negative Cotton effect and a substantial decline in the intensity of the spectrum. Compared with the case for the sample dissolved in methanol at pH 1, a change in the spectrum sign can additionally be observed in methanol at pH 12, with a positive Cotton effect occurring first. Therefore, it is possible to see a virtually total change in the CD spectrum sign depending on the pH of the environment. At this point, it can be postulated that, depending on whether FABT is dissolved in H_2O or in Mt−OH, the compound molecules exhibit different conformations at different pH values.

The next stage of the investigations involved analysis of FABT in the solutions using fluorescence spectroscopy methods. In analogy with crystals that were grown in the acidic environment, similar analyses were performed to elucidate the mechanisms of FABT dual fluorescence in the aqueous environment and single fluorescence in methanol. Figure 4 presents selected fluorescence emission spectra of

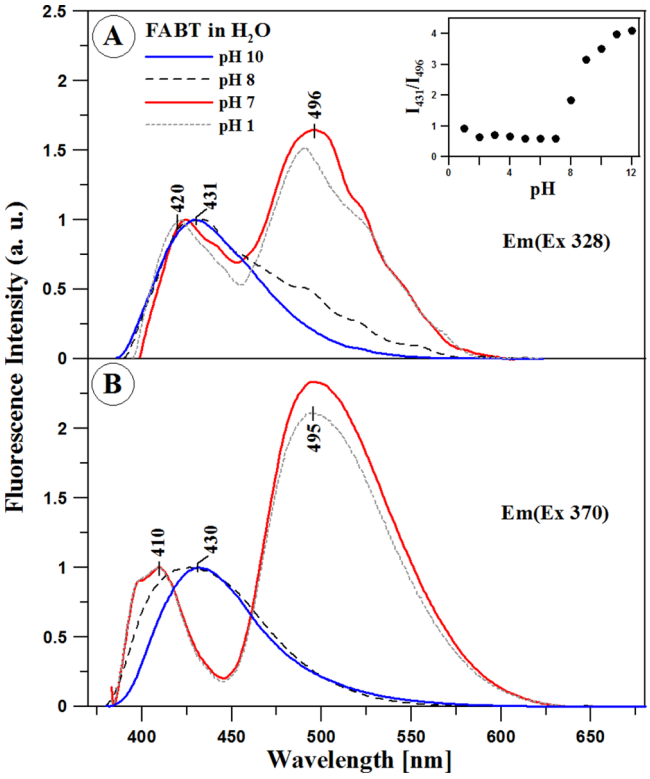

Figure 4. Panel A: fluorescence emission spectra of FABT obtained in the aqueous solution at different pH values (pH 10, solid blue line; pH 8, dotted black line; pH 7, solid red line; pH 1, dotted gray line). The excitation wavelength for all the spectra was 328 nm. Panel B presents similar spectra obtained at an excitation wavelength of 370 nm.

FABT in the aqueous solution obtained at different pH values (pH 1, 7, 8, and 10, respectively). The fluorescence emission spectra were normalized at a wavelength of ~420 nm for better visualization of the effect. In this case, the excitation wavelength for all the samples was 330 nm in panel A and 370 nm in panel B. As can be noticed, at pH 10, single fluorescence with a maximum at approximately 430 nm can be observed for both excitations. For pH 8, broadening of the emission spectrum can be seen. Next, additional fluorescence band with a maximum at 496 nm appears with decreasing pH (between pH 7 and 1) for both excitations. Furthermore, unlike the FABT spectra in the solutions, a ca. 100 nm shift in the emission spectra toward shorter wavelengths is observed for the crystals presented above. This effect is related to the considerably denser packing of FABT molecules in the crystal than in solutions, including the aggregates. Also in the case of the fluorescence emission spectra obtained for the excitation wavelength of 370 nm,

DOI: 10.1021/acs.jpca.5b06475
J. Phys. Chem. A XXXX, XXX, XXX−XXX

increased intensity in the second fluorescence band (~500 nm) and a slight shift of the first one toward shorter wavelengths can be clearly seen. However, for both excitations, a dual fluorescence effect with respective maxima at ca. 420 and 490 nm is visible.

The inset in Figure 4 presents the ratio of the FABT fluorescence maxima at a wavelength of 431 to 496 nm depending on the changes in the solution pH. As can be noticed, between pH 1 and pH 7, these peaks are arranged virtually in one horizontal line, likewise for the spectra presented in Figure 3 (panel A). This may imply that the process of nitrogen atom protonation is in equilibrium and does not change the value of the ratio (Scheme 1C). Above pH 7.5, the ratio increases substantially and the fluorescence at 496 nm disappears.

Figure 5 presents the FABT fluorescence excitation spectrum obtained in the aqueous solution at pH 1, 7, and 10 (panels A, C, and E, respectively) in comparison with the 1-T spectra (T = transmission) for the same samples. Panels B, D, and F show differential spectra (1-T)-(Ex). Emission was excited at 420 nm (pH 1), 430 nm (pH 7), and 496 nm (pH 12). In comparison with the 1-T spectra for both samples at pH 1 and pH 7, bands that should be assigned to aggregated forms of FABT molecules are observed in the case of the fluorescence excitation spectra. It can be noticed in panels A and B that the 1-T spectrum of FABT at pH 1 is hypsochromically shifted, whereas at pH 7 (panels C and D) a clear effect of a bathochromic shift is seen. According to the theory of exciton splitting, these shifts are related to two types of aggregation: the hypsochromic shift is associated with emergence of "card-pack" aggregates and the bathochromic shift is related to the head-to-tail aggregation type.[59,60] The considerable decrease in the bands related to aggregated forms in the alkaline environment (Figure 5) indicates FABT monomerisation in the solution. Therefore, it can be concluded that the dual fluorescence effect is not only associated with the molecular conformation "N" and "S" of FABT but also with the aggregation effects (probably dimers) in the aqueous solution. The results obtained using the RLS method, presented below, confirm this interpretation.

Figure 6 shows the results of fluorescence lifetime measurements for FABT in the aqueous solution in the entire pH range (shown for pH 1, 7, 8, and 12). Light with a wavelength of 372 nm was used for excitation. At pH 7, the selected excitation wavelength corresponds to the region of the ~338 nm absorption edge of the monomeric form and resonant excitation of the aggregated form (~370 nm). In turn, at a high pH value, ionized FABT monomers are subjected to resonance excitation (Figure 3A), whereas at a low pH aggregates undergo resonance excitation. The results were analyzed by deconvolution of fluorescence decay with the use of the apparatus profile and eq 1, separately for i = 1, 2, and 3 (i = number of the exponent). In all the analyzed cases, the double exponential model of fluorescence decay was optimal. The monoexponential decay model was insufficient, and addition of a third component did not improve the quality of the fit, which was verified by the value of the fit parameter and analysis of residue distribution. The first component of the fluorescence lifetimes was 0.64 ± 0.07 ns and remained constant along the pH range analyzed. The other component of the fluorescence decay was constant only for solutions with a pH lower than 8 and its value in such conditions was 1.81 ± 0.03 ns. An increase in pH over this value shortened the lifetime of this component in a monotonic mode and yielded a final value of 0.22 ns. The contributions of both components were almost equal for the low pH values, i.e., 0.46 ± 0.02 and 0.54 ± 0.02, respectively. For pH values higher than 6.5, a monotonic decrease in the first component was observed with the lowest value (0.15) at pH = 8.5. In turn, a further increase

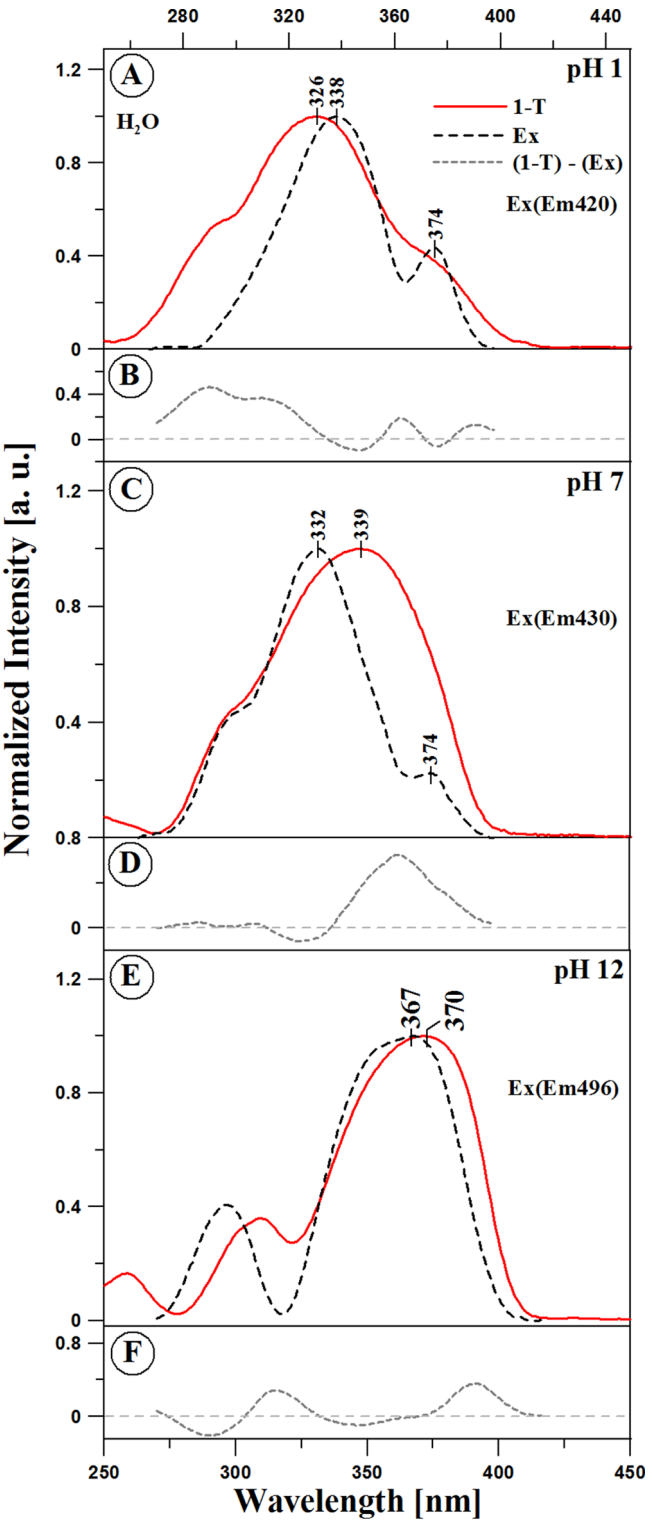

Figure 5. Fluorescence excitation spectra of FABT obtained in H_2O at pH 1 (panel A), pH 7 (panel C), and pH 12 (panel E) in comparison with 1-T spectra (T = transmission) in the same solvents. Panels B, D, and F show differential spectra (1-T)-(Ex). The excitation emission was recorded at wavelengths corresponding to the emission maximum.

DOI: 10.1021/acs.jpca.5b06475
J. Phys. Chem. A XXXX, XXX, XXX−XXX

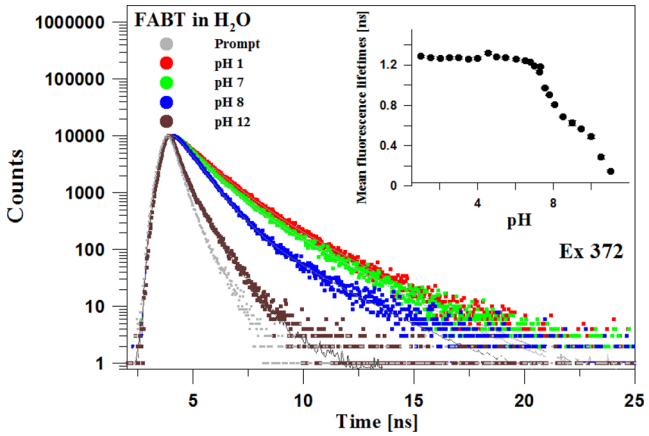

Figure 6. Effect of pH on the FABT fluorescence lifetime. Dotted lines show the decay of FABT fluorescence emission in water at the given pH, and solid lines are double exponential fits. The excitation pulse profile, set up at 372 nm, is shown by the dotted black line. The inset shows the dependence of the mean fluorescence lifetimes on pH.

in pH resulted in a higher contribution of the second fraction, which finally reached a value of 0.89. On the basis of the described components of fluorescence lifetimes and their contributions, average fluorescence lifetimes characteristic for each pH value were determined using eq 2. The relation between the average fluorescence lifetimes and pH of the solution is presented in the inset of Figure 6. The most important conclusion from these results is the observation that a decrease in the pH value is accompanied by a substantial increase in the fluorescence lifetime. In the pH range, in which single fluorescence is observed in the emission spectra, fluorescence lifetimes are considerably shortened to a value of ca. 0.45 ns. In contrast, in the region with dual fluorescence, a substantial increase in the average fluorescence lifetime to approximately 1.3 ns is found (see also Table 2). The effect of the fluorescence lifetime increase for conditions producing dual fluorescence is characteristic for excimer interactions,[61] in contrast to processes forced by the aggregation of molecules, where distinct shortening of the fluorescence lifetime or its complete disappearance is usually reported.

Further investigations involved fluorescence spectroscopy analysis of FABT dissolved in methanol. Figure 7 shows FABT fluorescence emission spectra obtained in methanol (panel D) and in the methanol solution acidified to pH 1 (apparent pH, panel C), as well as their respective excitation spectra superimposed on spectra 1-T (T = transmission) for Mt−OH at pH 1 (panel A) and pH 7 (apparent pH, panel B). The excitation wavelengths were 338 nm (blue lines in panels C and D) and 370 nm (dotted red line in panels C and D), respectively. The samples were prepared in the same conditions as those presented in Figure 3. As can be seen, in methanol single fluorescence of FABT is observed with a maximum at 407 nm (Figure 7, panel D). In turn, two independent fluorescence emission bands appear in the emission spectra of FABT dissolved in the methanol solution acidified to pH 1 at the excitation wavelengths of 338 and 370 nm: one at 407 nm (as for FABT dissolved in pure methanol) and the other one shifted considerably with a maximum at 505 nm (Figure 7, panel C). In this case, two separate fluorescence bands with overlapping emission regions are observed rather than the dual fluorescence described above. It should be noted that in the acidified methanol solution, the effect was observed at pH

Table 2. Fluorescence Lifetimes of FABT in H_2O in Relation to Changes in pH

pH	$\tau \pm \Delta\tau$ (ns)
1.0	1.286 ± 0.015
1.5	1.275 ± 0.012
2.01	1.269 ± 0.014
2.5	1.273 ± 0.014
3.0	1.271 ± 0.014
3.53	1.263 ± 0.012
4.0	1.269 ± 0.013
4.54	1.320 ± 0.015
5.01	1.282 ± 0.011
5.46	1.271 ± 0.012
6.03	1.258 ± 0.013
6.52	1.244 ± 0.012
6.78	1.232 ± 0.012
7.01	1.189 ± 0.012
7.26	1.134 ± 0.011
7.32	1.186 ± 0.011
7.55	1.977 ± 0.009
7.78	1.903 ± 0.007
8.06	1.808 ± 0.007
8.5	1.687 ± 0.006
9.0	1.627 ± 0.03
9.46	0.567 ± 0.012
10	0.488 ± 0.02
10.53	0.288 ± 0.022
11.02	0.150 ± 0.012
11.51	0.126 ± 0.006
12	0.264 ± 0.004

ranging from 2 to 1. It is known from crystallographic data that $FABTH^+$ was in the "S" conformation in the Mt−OH solvate, Scheme 1D.

Panels A and B of Figure 7 present fluorescence excitation spectra in comparison with their 1-T spectra. Panel A shows characteristic bands on the long wavelength side of the spectrum with a maximum at 374 nm. This effect is characteristic for processes of molecular aggregation. The excitation and 1-T spectra shown in panel B are only insignificantly shifted relative to each other and single emission is visible in the fluorescence emission spectra.

Effect of Temperature on Fluorescence Spectra. Figure 8, panel A, shows electronic absorption spectra of FABT dissolved in water depending on changes in the ambient temperature. It is evident that an increase in the temperature causes a decline in absorbance of the band with a maximum at approximately 340 nm and its slight 3 nm blue shift. Noteworthy, besides the change in absorbance, no significant changes in the FABT spectrum can be observed in this case. The inset in Figure 8 presents the correlation between the intensity of the absorption maximum band at ca. 340 nm and the temperature of the sample. An effect of a drop of the absorbance maximum with increasing temperature is clearly visible. This decline is probably related to thermally induced deaggregation of the sample. This implies that, as shown in Figure 5, the spectrum of the monomeric FABT form is underpinned by the aggregated forms of the compound.

In the subsequent part of the investigations, the impact of temperature on the dual fluorescence effect was analyzed. The panel on the left in Figure 8 (panels B and D) shows selected spectra measured in increasing temperature, whereas spectra

DOI: 10.1021/acs.jpca.5b06475
J. Phys. Chem. A XXXX, XXX, XXX−XXX

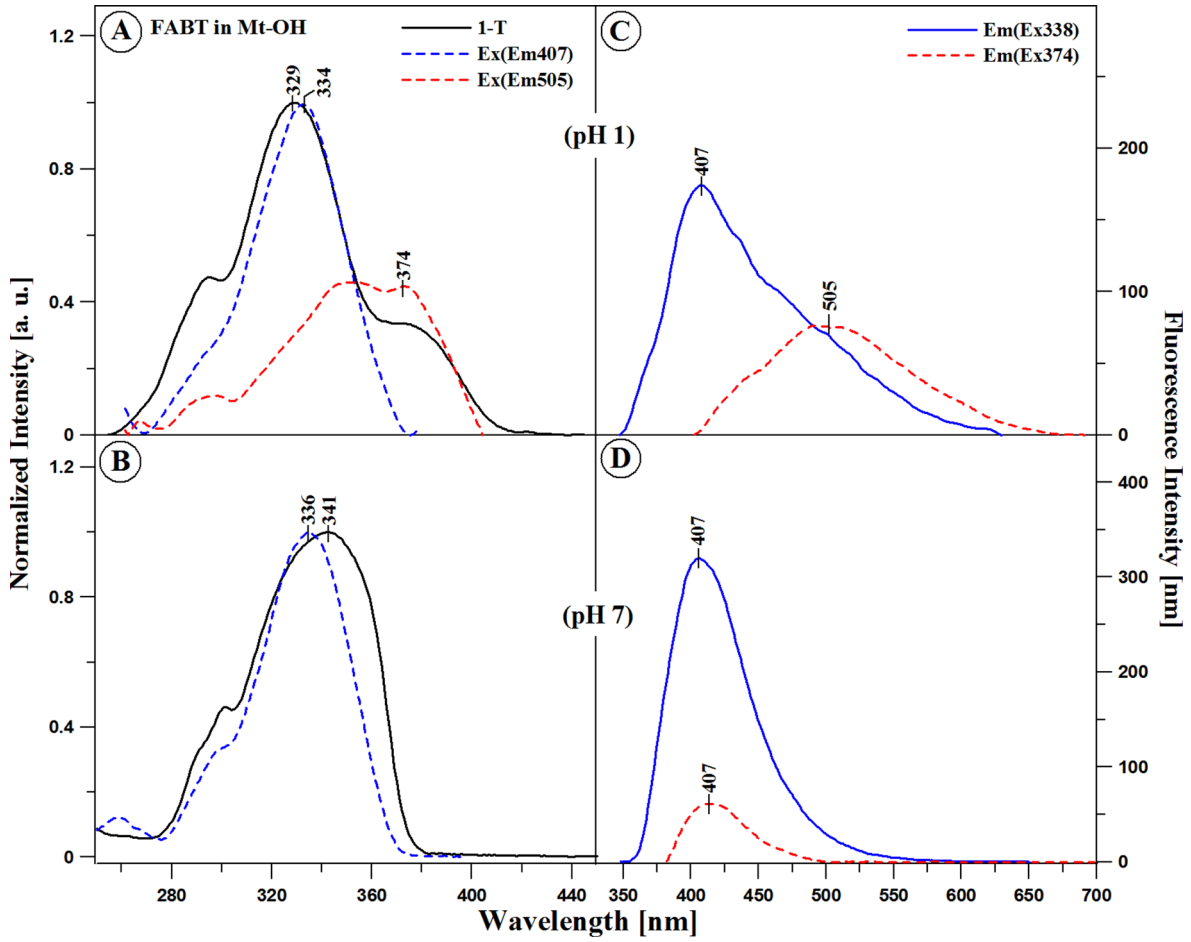

Figure 7. Panels A and B: fluorescence excitation spectra of FABT in Mt−OH at pH 1 (panel A) and pH 7 (panel B) in comparison with 1-T spectra (T = transmission). Panels C and D present fluorescence emission spectra of FABT obtained in methanol (panel D) and in methanol solution acidified to pH 1 (panel C). The excitation wavelengths for the spectra in both panels were 328 nm (blue lines) and 374 nm (red lines).

measured in decreasing temperature are presented in the panel on the right. It can be noticed that the temperature rise causes a decrease in the intensity of the second fluorescence band (with a maximum at 496 nm), which is also clearly indicated in the inset in Figure 8 (between panels B and D), showing a correlation between the ratio of the fluorescence maxima at 420−496 nm and the temperature. There is a distinct effect of the decrease in the intensity of the second fluorescence component and a decline in the fluorescence intensity band at 420 nm. The adjacent panel presents FABT fluorescence emission spectra along the decreasing temperature of the aqueous solution. Contrary to the expectations, it is evident that, together with cooling of the sample, the band at the wavelength of ca. 496 nm does not regain its former intensity. Therefore, single fluorescence is emitted after heating and cooling of the FABT sample in the aqueous solution. This effect can be explained by the impact of temperature on deaggregation of the molecules followed by rotation of the resorcyl ring caused by H_2O interaction. Because no band at 496 nm is observed after lowering the temperature of the aqueous solution to the initial band state, a question may arise whether there is any thermal damage to the FABT molecule. To clarify this issue, an experiment was carried out, in which 0.1 M NaOH and HCl were consecutively added to an FABT sample dissolved in an aqueous solution heated to 90 °C and cooled to room temperature. Figure 8 (panel C) shows FABT absorption spectra in the aqueous solution at pH 5.5 and 20 °C (dotted blue line). The solution was heated to a temperature of 85 °C and next cooled to 20 °C. In the next step, the pH of the solution was increased to 12 by addition of 0.1 M NaOH, which gave a spectrum similar to that in Figure 3 (panel A, spectrum at pH 12). Acidification of the solution yielded a spectrum that was identical to that presented in Figure 3 (panel A, spectrum at pH 1).

Figure 8 (panel E) presents FABT fluorescence emission spectra obtained in the aqueous solution in exactly the same conditions as those shown in panel C. The excitation wavelength for both spectra was 330 nm. Clearly, single fluorescence is observed in the case of the FABT emission spectrum after addition of NaOH (red line). In contrast, after addition of HCl (pH 1) to the sample, dual fluorescence with a maximum at 416 and 496 nm appears. On the basis of these results, it can be concluded that heating can lead to breaking of the hydrogen bond between the −OH group (in the *ortho* positon) from the resorcyl ring and the nitrogen atom from the thiadiazole ring (Scheme 1C), which facilitates rotation of the resorcyl ring and adoption of conformation "S". Another alkalization step results in dissociation of protons, which restores conformation "N" after acidification.

The TCSPC method was also used for analyzing the impact of temperature on fluorescence decay in the aqueous solution of FABT. The experiments were carried out at pH 7 in the

DOI: 10.1021/acs.jpca.5b06475
J. Phys. Chem. A XXXX, XXX, XXX−XXX

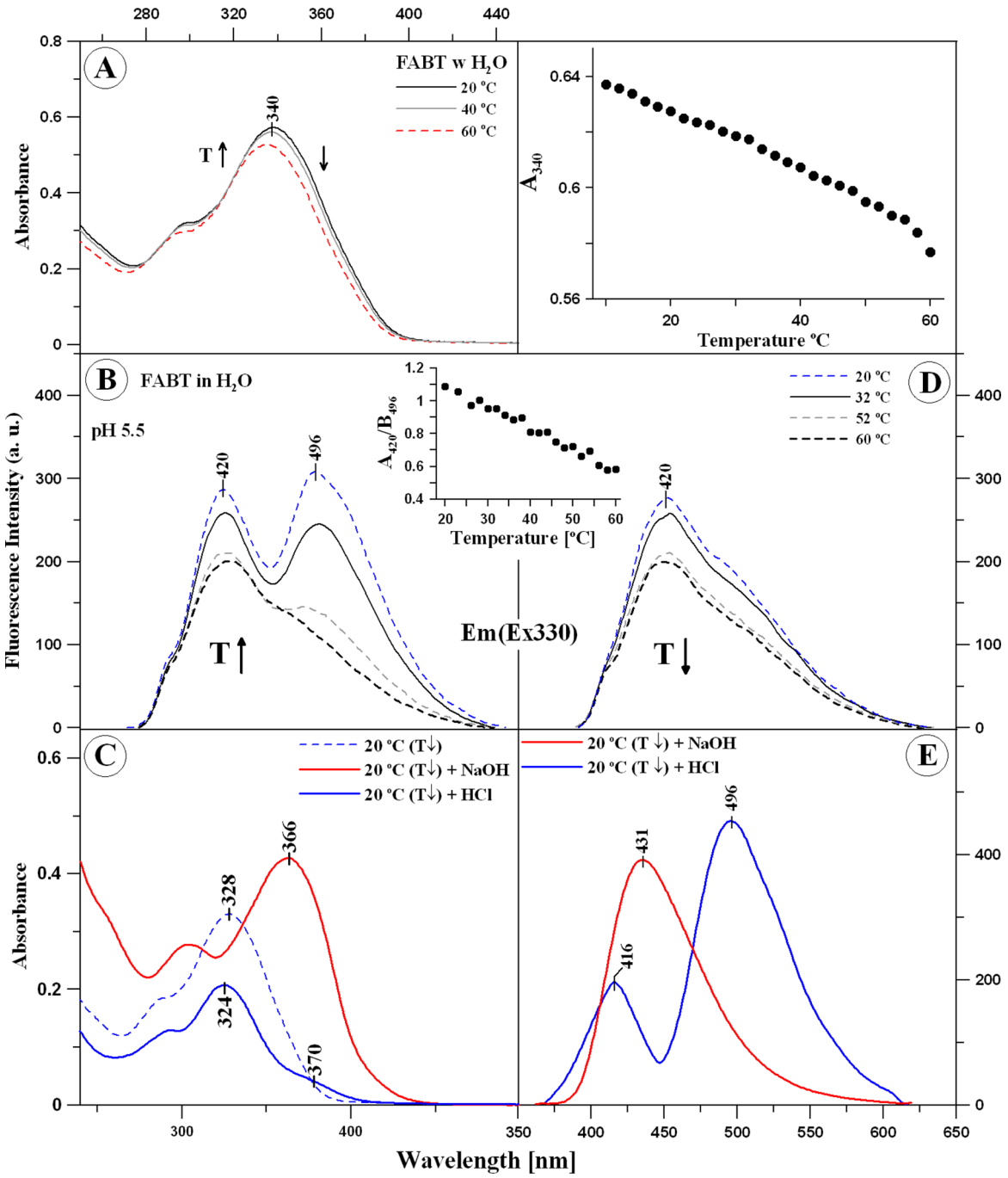

Figure 8. Panel A: electron absorption spectra of FABT in H_2O obtained at different temperature values (from 10 to 60 °C). The inset presents the dependence of the absorption intensity at a wavelength of 340 nm on temperature changes (panels B and D). Fluorescence emission spectra of FABT obtained in the aqueous solution at pH 5.5 at different temperatures. The excitation wavelength for all the spectra was 330 nm. Panel B shows spectra accompanying the temperature rise, and panel D presents spectra along the decreasing temperature. The inset between panels B and D shows the dependence of the fluorescence intensity maximum at 420 to 496 nm on temperature changes. Panel C presents electron absorption spectra of FABT obtained in the aqueous solution at pH 5.5 and a temperature of 20 °C (dotted blue line). Next, after heating to 85 °C and lowering the temperature to 20 °C, 0.1 M NaOH was added (solid red line), thereby achieving pH 12 and 0.1 M HCl (solid blue line) to obtain pH 1. Panel E shows fluorescence emission spectra of FABT obtained in the aqueous solution in conditions similar to those presented in panel C. The excitation wavelength for both spectra was 330 nm.

same way as for the pH dependence described above (Figure 6, Table 3). The measurements were performed in temperatures from 20 to 85 °C; next, the sample was cooled again to 20 °C. The rise in the temperature was accompanied by monotonic shortening of both components of fluorescence decay from 0.59 and 1.8 ns for 20 °C to 0.05 and 0.46 for 85 °C. The intensities of both fractions also underwent monotonic changes. An increase to a value of 95% was noticed for the first, shorter component. Reverse changes were observed during cooling, i.e., an increase in both component lifetimes and reduced contribution of the shorter decay component. For the initial temperature of 20 °C, the contribution reached the initial values; however, the component fluorescence lifetimes did not reach them and were 0.14 and 0.64 ns, respectively. The

DOI: 10.1021/acs.jpca.5b06475
J. Phys. Chem. A XXXX, XXX, XXX−XXX

Table 3. Fluorescence Lifetimes of FABT in H_2O in Relation to Changes in Temperature (20−90 °C)

	temp (°C)	$\tau \pm \Delta\tau$ (ns)
$T\uparrow$	20	1.095 ± 0.011
	30	1.021 ± 0.011
	40	0.851 ± 0.010
	50	0.332 ± 0.006
	55	0.291 ± 0.010
	60	0.303 ± 0.006
	65	0.230 ± 0.005
	70	0.159 ± 0.011
	75	0.085 ± 0.004
	80	0.004 ± 0.044
	85	0.077 ± 0.004
$T\downarrow$	75	0.006 ± 0.001
	70	0.003 ± 0.097
	65	0.054 ± 0.003
	60	0.056 ± 0.004
	55	0.085 ± 0.004
	50	0.083 ± 0.005
	40	0.104 ± 0.009
	35	0.148 ± 0.027
	30	0.397 ± 0.052
	7.5	0.557 ± 0.024

average fluorescence lifetime expressed with eq 2 was used for presentation of the described temperature dependence and shown in the inset in Figure 9. In summary, the distinct increase in the fluorescence lifetime in the temperature range characteristic for the dual fluorescence effect should be emphasized.

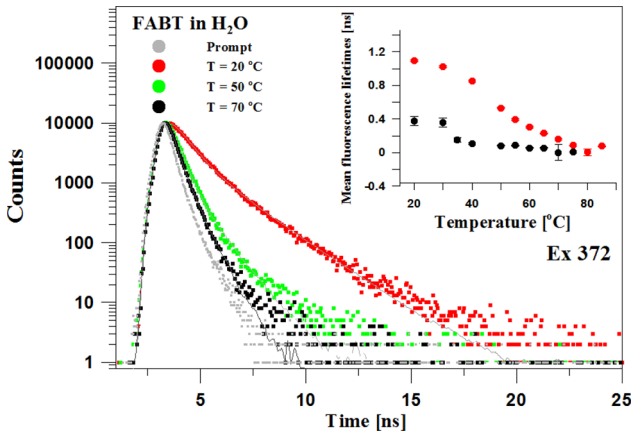

Figure 9. Effect of temperature on the FABT fluorescence lifetime. Dotted lines show the decay of FABT fluorescence emission in water at the given temperature, and solid lines are double exponential fits. The excitation pulse profile, set up at 372 nm, is shown by the dotted black line. The inset shows the dependence of the mean fluorescence lifetimes on temperature, observed at an increasing (black circles) or decreasing (red circles) temperature.

Next, to investigate the impact of aggregation on the dual fluorescence effect, RLS spectra were obtained for FABT dissolved in water depending on changes in the ambient temperature. Figure 10 (panel A) shows RLS spectra of FABT obtained in the aqueous solution at pH 5.5 and a rising temperature. In turn, panel B presents RLS spectra of FABT obtained in the aqueous solution at pH 5.5 and a temperature

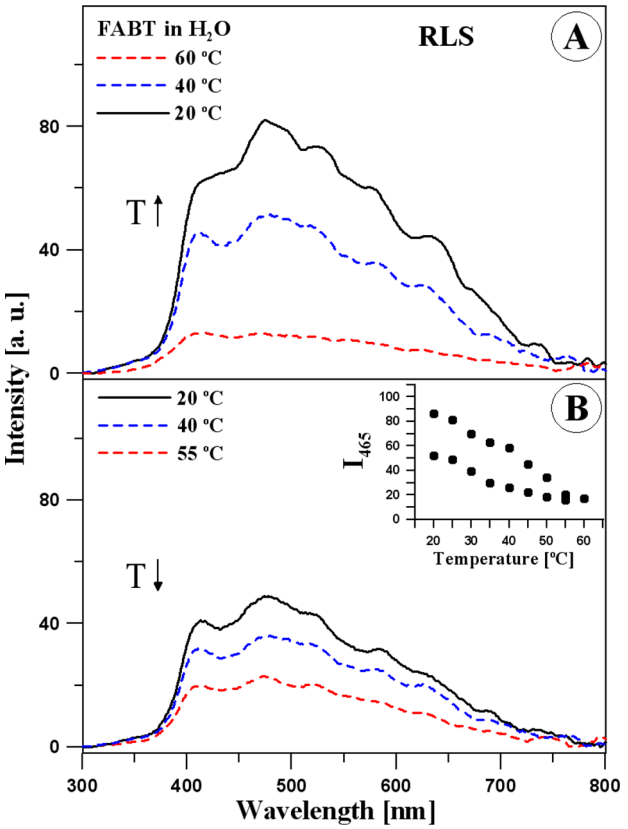

Figure 10. RLS (resonance light scattering) spectra of FABT obtained in the aqueous solution at pH 5.5 and different temperatures. Panels A and B show RLS spectra with an increasing and decreasing temperature, respectively. The inset in panel B presents the ratio of RLS signal intensity at a wavelength of 465 nm and temperature changes.

decreasing to its initial value. The occurrence of RLS bands should be assigned to chromophore aggregation of components contained in the solution.[53,54] As can be seen, RLS bands with higher or lower intensity are present in water at different values of temperature. A decline in the intensity of the RLS bands along the temperature increase is evident. It can be seen in panel B that the intensity of the RLS spectra does not return to the baseline value along the temperature decline. To sum up, it should be noted that the RLS bands related to chromophore aggregation of the FABT molecules are not specific and cannot fully explain the phenomenon of the FABT dual fluorescence in the aqueous solution or the phenomenon of the two separate emissions in the methanol solution. Distinct RLS bands can be observed in the case of FABT both in methanol (not shown) and in the aqueous solution; however, during the return to the dual fluorescence effect in the case of the RLS spectra of FABT dissolved in the aqueous solution, the increase in pH was accompanied by a decline in the RLS band intensity (not shown). The vibrational structure of RLS bands implies the presence of multiple aggregated FABT structures differing in their size.[50] The inset in Figure 10 shows the dependence of the band intensity at 465 nm from the RLS spectra of FABT dissolved in water on temperature. It can be noticed that the increase in the ambient temperature is accompanied by reduction of band intensity at 465 nm, which does not return to the initial value after temperature lowering.

DOI: 10.1021/acs.jpca.5b06475
J. Phys. Chem. A XXXX, XXX, XXX−XXX

Raman Spectroscopy from FABT Solutions. Similar to the case for the Raman spectra of the FABT monocrystals (Figure 2), in the case of the solutions, substantial changes in the Raman spectra of FABT dissolved in the aqueous and methanol solutions at pH 1 can be noticed. Figure 2 (panel C) presents Raman spectra of FABT from the aqueous (red line) and methanol (dashed black line) solutions. The samples were excited with a wavelength of 785 nm at a temperature of 22 °C. To facilitate further discussion, Table 1 contains a list of the locations of the main Raman bands of FABT. As can be observed, in comparison of the Raman spectra of FABT obtained from the methanol solvate with the Raman spectra of FABT samples taken from the aqueous solution, new bands appear with a maximum at 1553, 1505, 1490, 1395, 1331, and 1258 cm^{-1}. The bands are characteristic for stretching vibrations of the C═C, C═N, C—C, and C—H groups in the aromatic ring.

The aforementioned change in the position of the −OH group from the resorcyl ring (in the *ortho* positon) relative to the 1,3,4-thiadiazole system exerts an impact on the changes observed in the FABT Raman spectra. The bands observed for FABT dissolved in water and totally invisible in methanol seem to be most important for elucidation of the dual fluorescence effect in the FABT molecule. These bands, with maxima at 1505 and 1490 cm^{-1}, correspond (as already mentioned in the presentation of the Raman spectra of the crystal forms) to C═N stretching vibrations and very intense C—C stretching vibrations between the thiadiazole and resorcinol rings. Comparison of the presented Raman spectra of FABT in the solutions (Figure 2, panel C) with these for monocrystals (Figure 2A,B) clearly indicates that the conformation of FABT molecules plays a pivotal role in elucidation of the mechanisms of the dual fluorescence phenomenon.

CONCLUSIONS

The fluorescence spectroscopy investigations presented in the paper indicate appearance of dual fluorescence in the FABT emission spectrum in the aqueous solution. The phenomenon analyzed in FABT monocrystals implies dependence of this effect on the "N" conformation of the resorcyl ring (the −OH group from the resorcyl ring oriented toward the nitrogen atom from the 1,3,4-thiadiazole ring due to 180° rotation). The measurements of the FABT fluorescence spectra in the solution with different concentrations of hydrogen ions reveal appearance of the analyzed effect at pH values ranging from 1 to 7. The RLS analyses indicate an impact of chromophore aggregation on the dual fluorescence effect for FABT in the aqueous solution. The phenomenon of the dual fluorescence of FABT molecules depends on the specific "N" conformation of the compound molecules and FABT chromophore aggregation, which forces intramolecular interactions in the analyzed system. The specific molecule conformation ("N") is characterized by distinct shortening of the bond between the C atoms from the resorcinol and 1,3,4-thiadiazole rings in combination with aggregation of the system. The investigations described above will facilitate fast analysis of conformational effects, which will allow identification of structural changes in 1,3,4-thiadiazoles using the fluorescence spectroscopy technique in different molecular systems. Especially in biological systems, fast determination of the thiadiazole conformation can help in understanding its in situ biological activity.

ASSOCIATED CONTENT

Supporting Information

The Supporting Information is available free of charge on the ACS Publications website at DOI: 10.1021/acs.jpca.5b06475.

pH-metric titration curve for FABT, Raman spectra calculations and scattering activities and crystallographic structures (PDF)

AUTHOR INFORMATION

Corresponding Authors

*A. Matwijczuk. Fax: +(48 81) 4456684. Phone: +(48 81) 445 69 37. E-mail: arkadiusz.matwijczuk@up.lublin.pl, arekmatwijczuk@gmail.com.

*M. Gagoś. Phone: +(48 81) 537 59 04. E-mail: mariusz.gagos@poczta.umcs.lublin.pl.

Notes

The authors declare no competing financial interest.

REFERENCES

(1) Jain, A. K.; Sharma, S.; Vaidya, A.; Ravichandran, V.; Agrawal, R. K. 1,3,4-Thiadiazole and Its Derivatives: A Review on Recent Progress in Biological Activities. *Chem. Biol. Drug Des.* **2013**, *81*, 557−576.

(2) Farghaly, T. A.; Abdallah, M. A.; Muhammad, Z. A. Synthesis and Evaluation of the Anti-Microbial Activity of New Heterocycles Containing the 1,3,4-Thiadiazole Moiety. *Molecules* **2011**, *16*, 10420−10432.

(3) Barboiu, M.; Cimpoesu, M.; Guran, C.; Supuran, C. T. 1,3,4-Thiadiazole Derivatives. Part 9. Synthesis and Biological Activity of Metal Complexes of 5-(2-Aminoethyl)-2-Amino-1,3,4-Thiadiazole. *Met Based Drugs* **1996**, *3*, 227−32.

(4) Jitianu, A.; Llies, M. A.; Briganti, F.; Scozzafava, A.; Supuran, C. T. Complexes with Biologically Active Ligands. Part 9 Metal Complexes of 5-Benzoylamino- and 5-(3-Nitrobenzoyl-Amino)-1,3,4-Thiadiazole-2-Sulfonamide as Carbonic Anhydrase Inhibitors. *Met Based Drugs* **1997**, *4*, 1−7.

(5) Supuran, C. T.; Scozzafava, A.; Briganti, F.; Ilies, M. A.; Jitianu, A. Carbonic Anhydrase Inhibitors. Part 55 Metal Complexes of 1,3,4-Thiadiazole-2-Sulfonamide Derivatives: In Vitro Inhibition Studies with Carbonic Anhydrase Isozymes I, Ii and Iv. *Met Based Drugs* **1998**, *5*, 103−14.

(6) Turan, N.; Topcu, M. F.; Ergin, Z.; Sandal, S.; Tuzcu, M.; Akpolat, N.; Yilmaz, B.; Sekerci, M.; Karatepe, M. Pro-Oxidant and Antiproliferative Effects of the 1,3,4-Thiadiazole-Based Schiff Base and Its Metal Complexes. *Drug Chem. Toxicol.* **2011**, *34*, 369−378.

(7) Chabner, B. A.; Roberts, T. G., Jr. Timeline: Chemotherapy and the War on Cancer. *Nat. Rev. Cancer* **2005**, *5*, 65−72.

(8) Rajak, H.; Deshmukh, R.; Aggarwal, N.; Kashaw, S.; Kharya, M. D.; Mishra, P. Synthesis of Novel 2,5-Disubstituted 1,3,4-Thiadiazoles for Their Potential Anticonvulsant Activity: Pharmacophoric Model Studies. *Arch. Pharm. (Weinheim, Ger.)* **2009**, *342*, 453−61.

(9) Li, Y.; Geng, J.; Liu, Y.; Yu, S.; Zhao, G. Thiadiazole-a Promising Structure in Medicinal Chemistry. *ChemMedChem* **2013**, *8*, 27−41.

(10) Matysiak, J.; Nasulewicz, A.; Pełczyńska, M.; Świtalska, M.; Jaroszewicz, I.; Opolski, A. Synthesis And antiproliferative Activity Of some 5-Substituted 2-(2,4-Dihydroxyphenyl)-1,3,4-Thiadiazoles. *Eur. J. Med. Chem.* **2006**, *41*, 475−482.

(11) Cressier, D.; Prouillac, C.; Hernandez, P.; Amourette, C.; Diserbo, M.; Lion, C.; Rima, G. Synthesis, Antioxidant Properties and Radioprotective Effects of New Benzothiazoles and Thiadiazoles. *Bioorg. Med. Chem.* **2009**, *17*, 5275−84.

(12) Kaminski, D. M.; Matwijczuk, A.; Pociecha, D.; Gorecka, E.; Niewiadomy, A.; Dmowska, M.; Gagoś, M. Effect of 2-(4-Fluorophenylamino)-5-(2,4-Dihydroxyphenyl)-1,3,4-Thiadiazole on the Molecular Organisation and Structural Properties of the Dppc Lipid Multibilayers. *Biochim. Biophys. Acta, Biomembr.* **2012**, *1818*, 2850−9.

DOI: 10.1021/acs.jpca.5b06475
J. Phys. Chem. A XXXX, XXX, XXX−XXX

(13) Matwijczuk, A.; Gorecki, A.; Kaminski, D.; Mysliwa-Kurdziel, B.; Fiedor, L.; Niewiadomy, A.; Karwasz, G. P.; Gagoś, M. Influence of Solvent Polarizability on the Keto-Enol Equilibrium in 4-[5-(Naphthalen-1-Ylmethyl)-1,3,4-Thiadiazol-2-Yl]Benzene-1,3-Diol. *J. Fluoresc.* **2015**, DOI: 10.1007/s10895-015-1679-x.
(14) Gagoś, M.; Matwijczuk, A.; Kaminski, D.; Niewiadomy, A.; Kowalski, R.; Karwasz, G. P. Spectroscopic Studies of Intramolecular Proton Transfer in 2-(4-Fluorophenylamino)-5-(2,4-Dihydroxybenzeno)-1,3,4-Thiadiazole. *J. Fluoresc.* **2011**, *21*, 1−10.
(15) Panja, S.; Chakravorti, S. Dynamics of Twisted Intramolecular Charge Transfer Process of 4-N,N-Dimethylaminocinnamic Acid in a-Cyclodextrin Environment. *Chem. Phys. Lett.* **2001**, *336*, 57−64.
(16) Matsushita, Y.; Hikida, T. The Effect of Cyclodextrin Complexation on the Fluorescence Properties of Ethyl-4′-Dimethylaminobenzoate. *Chem. Phys. Lett.* **1999**, *313*, 85−90.
(17) Ramalingam, A.; Sivaram, B. M.; Palanisamy, P. K.; Masilamani, V. Photophysics of Tict States of 7-Diethylamino-4-Methyl Coumarin Dye by Energy Transfer Techniques. Spectrochimica Acta Part A. *Spectrochim. Acta, Part A* **2000**, *56*, 1205−1210.
(18) Chen, L.; Zhang, X.; Zhang, C.; Zhou, G.; Zhang, W.; Xiang, D.; He, Z.; Wang, H. Dual-Color Fluorescence and Homogeneous Immunoassay for the Determination of Human Enterovirus 71. *Anal. Chem.* **2011**, *83*, 7316−22.
(19) Brancato, G.; Signore, G.; Neyroz, P.; Polli, D.; Cerullo, G.; Abbandonato, G.; Nucara, L.; Barone, V.; Beltram, F.; Bizzarri, R. Dual Fluorescence through Kasha's Rule Breaking: An Unconventional Photomechanism for Intracellular Probe Design. *J. Phys. Chem. B* **2015**, *119*, 6144−54.
(20) Tanaka, H.; Shizu, K.; Nakanotani, H.; Adachi, C. Dual Intramolecular Charge-Transfer Fluorescence Derived from a Phenothiazine-Triphenyltriazine Derivative. *J. Phys. Chem. C* **2014**, *118*, 15985−15994.
(21) Ozawa, R.; Hayashita, T.; Matsui, T.; Nakayama, C.; Yamauchi, A.; Suzuki, I. Effects of Cyclodextrins and Saccharides on Dual Fluorescence of N,N-Dimethyl-4-Aminophenylboronic Acid in Water. *J. Inclusion Phenom. Mol. Recognit. Chem.* **2008**, *60*, 253−261.
(22) Chattopadhyay, A. K.; Basu, S.; Chakraborty, S. C. Temperature Dependent Dual Luminescence of 9-Chloro-10, 10′-Bis-(Dichloromethyleno)-(9′H)-10,10′-Dihydro-9, 9′-Bianthryl (Cddb) and Its Excited State Dipole Moment. *J. Lumin.* **1995**, *65*, 269−277.
(23) Albinsson, B. Dual Fluorescence from N6,N6-Dimethyladenosine. *J. Am. Chem. Soc.* **1997**, *119*, 6369−6375.
(24) Catalan, J.; Perez, P.; Laynez, J.; Blanco, F. G. Analysis of the Solvent Effect on the Photophysics Properties of 6-Propionyl-2-(Dimethylamino)Naphthalene (Prodan). *J. Fluoresc.* **1991**, *1*, 215−223.
(25) Murali, S.; Changenet-Barret, P.; Ley, C.; Plaza, P.; Rettig, W.; Martin, M. M.; Lapouyade, R. Photophysical Properties of Pyrrolobenzenes with Different Linking and Substitution Pattern: The Transition between Charge Transfer States with Large (Mict) and Small (Tict) Resonance Interaction. *Chem. Phys. Lett.* **2005**, *411*, 192−197.
(26) Yang, J.-S.; Lin, C.-K.; Lahoti, A. M.; Tseng, C.-K.; Liu, Y.-H.; Lee, G.-H.; Peng, S.-M. Effect of Ground-State Twisting on the Trans → Cis Photoisomerization and Tict State Formation of Aminostilbenes§. *J. Phys. Chem. A* **2009**, *113*, 4868−4877.
(27) Choi, L.-S. Triple Fluorescence of 4-(1,4,8,11-Tetraazacyclotetradecyl)Benzonitrile. *Chem. Commun.* **1998**, 893−894.
(28) Matsushita, Y.; Hikida, T. Tict State Formation in the 4′-Dimethylaminoacetophenone−A-Cyclodexdtrin Inclusion Complex. *Chem. Phys. Lett.* **1998**, *290*, 349−354.
(29) Jiang, Y.-B. Twisted Intramolecular Charge Transfer of Methyl P-Dimethylaminobenzoate in Aqueous B-Cyclodextrin Solution. *Spectrochim. Acta, Part A* **1995**, *51*, 275−282.
(30) Dey, J.; Warner, I. M. Dual Fluorescence of 9-(N,N-Dimethylamino)Anthracene: Effect of Solvent Polarity and Viscosity. *J. Phys. Chem. A* **1997**, *101*, 4872−4878.
(31) Patil, V.; Padalkar, V.; Tathe, A.; Gupta, V.; Sekar, N. Synthesis, Photo-Physical and Dft Studies of Esipt Inspired Novel 2-(2′,4′-Dihydroxyphenyl) Benzimidazole, Benzoxazole and Benzothiazole. *J. Fluoresc.* **2013**, *23*, 1019−1029.
(32) Murali, S.; Kharlanov, V.; Rettig, W.; Tolmachev, A. I.; Kropachev, A. V. The Tetrafluoro Analogue of Dmabn: Anomalous Fluorescence and Mechanistic Considerations. *J. Phys. Chem. A* **2005**, *109*, 6420−6429.
(33) Shcherban', T. P.; Granchak, V. M.; Sakhno, T. V.; Khakhel', O. A. Conformational Mobility of 4,4′-Bisdimethyl-Aminobenzophenone in the Excited State. *Theor. Exp. Chem.* **2005**, *41* (41), 198−202.
(34) Rodembusch, F. S.; Leusin, F. P.; Campo, L. F.; Stefani, V. Excited State Intramolecular Proton Transfer in Amino 2-(2′-Hydroxyphenyl)Benzazole Derivatives: Effects of the Solvent and the Amino Group Position. *J. Lumin.* **2007**, *126*, 728−734.
(35) Nie, D.; Bian, Z.; Yu, A.; Chen, Z.; Liu, Z.; Huang, C. Ground and Excited State Intramolecular Proton Transfer Controlled Intramolecular Charge Separation and Recombination: A New Type of Charge and Proton Transfer Reaction. *Chem. Phys.* **2008**, *348*, 181−186.
(36) Marri, E.; Galiazzo, G.; Mazzucato, U.; Spalletti, A. Effect of Solvent Polarizability on Dual Fluorescence of Ee-1-Phenyl,4-(1′-Pyrenyl)-1,3-Butadiene. *Chem. Phys.* **2000**, *260*, 383−390.
(37) Abella, C. A. M.; Rodembusch, F. S.; Stefani, V. Synthesis of Novel Tröger's Bases Analogues. The First Ones Fluorescent by Excited State Intramolecular Proton Transfer (Esipt). *Tetrahedron Lett.* **2004**, *45*, 5601−5604.
(38) Dennison, S. M.; Guharay, J.; Sengupta, P. K. Excited-State Intramolecular Proton Transfer (Esipt) and Charge Transfer (Ct) Fluorescence Probe for Model Membranes. Spectrochimica Acta Part A. *Spectrochim. Acta, Part A* **1999**, *55*, 1127−1132.
(39) Oncul, S.; Demchenko, A. P. The Effects of Thermal Quenching on the Excited-State Intramolecular Proton Transfer Reaction in 3-Hydroxyflavones. Spectrochimica Acta Part A. *Spectrochim. Acta, Part A* **2006**, *65*, 179−183.
(40) Chuang, W.-T.; Hsieh, C.-C.; Lai, C.-H.; Lai, C.-H.; Shih, C.-W.; Chen, K.-Y.; Hung, W.-Y.; Hsu, Y.-H.; Chou, P.-T. Excited-State Intramolecular Proton Transfer Molecules Bearing O-Hydroxy Analogues of Green Fluorescent Protein Chromophore. *J. Org. Chem.* **2011**, *76*, 8189−8202.
(41) Fang, S.-K.; Tsai, H.-Y.; Hu, J.-W.; Chen, K.-Y. A White-Light-Emitting Small Molecule: Synthesis, Crystal Structure, and Optical Properties. *Int. J. Photoenergy* **2014**, *2014*, 124753.
(42) Sakai, K.-i.; Kawamura, H.; Kobayashi, N.; Ishikawa, T.; Ikeda, C.; Kikuchi, T.; Akutagawa, T. Highly Efficient Solid-State Red Fluorophores Using Esipt: Crystal Packing and Fluorescence Properties of Alkoxy-Substituted Dibenzothiazolylphenols. *CrystEngComm* **2014**, *16*, 3180−3185.
(43) Yang, W.; Chen, X. Dual Fluorescence of Excited State Intra-Molecular Proton Transfer of Hbfo: Mechanistic Understanding, Substituent and Solvent Effects. *Phys. Chem. Chem. Phys.* **2014**, *16*, 4242−4250.
(44) Temperini, C.; Cecchi, A.; Boyle, N. A.; Scozzafava, A.; Escribano Cabeza, J.; Wentworth, P.; Blackburn, G. M.; Supuran, C. T. Carbonic Anhydrase Inhibitors. Interaction of 2-N,N-Dimethylamino-1,3,4-Thiadiazole-5-Methanesulfonamide with 12 Mammalian Isoforms: Kinetic and X-Ray Crystallographic Studies. *Bioorg. Med. Chem. Lett.* **2008**, *18*, 999−1005.
(45) Menchise, V.; De Simone, G.; Di Fiore, A.; Scozzafava, A.; Supuran, C. T. Carbonic Anhydrase Inhibitors: X-Ray Crystallographic Studies for the Binding of 5-Amino-1,3,4-Thiadiazole-2-Sulfonamide and 5-(4-Amino-3-Chloro-5-Fluorophenylsulfonamido)1,3,4-Thiadiazole-2-Sulfonamide to Human Isoform Ii. *Bioorg. Med. Chem. Lett.* **2006**, *16*, 6204−6208.
(46) Bourhis, J. M.; Vignaud, C.; Pietrancosta, N.; Gueritte, F.; Guenard, D.; Lederer, F.; Lindqvist, Y. Structure of Human Glycolate Oxidase in Complex with the Inhibitor 4-Carboxy-5-[(4-Chlorophenyl)Sulfanyl]-1,2,3-Thiadiazole. *Acta Crystallogr., Sect. F: Struct. Biol. Cryst. Commun.* **2009**, *65*, 1246−1253.
(47) Sharp, S. Y.; Roe, S. M.; Kazlauskas, E.; Cikotiene, I.; Workman, P.; Matulis, D.; Prodromou, C. Co-Crystalization and in Vitro

DOI: 10.1021/acs.jpca.5b06475
J. Phys. Chem. A XXXX, XXX, XXX−XXX

Biological Characterization of 5-Aryl-4-(5-Substituted-2−4-Dihydroxyphenyl)-1,2,3-Thiadiazole Hsp90 Inhibitors. *PLoS One* **2012**, *7*, e44642.
(48) Hoser, A. A.; Kaminski, D. M.; Matwijczuk, A.; Niewiadomy, A.; Gagoś, M.; Wozniak, K. On Polymorphism of 2-(4-Fluorophenylamino)-5-(2,4-Dihydroxybenzeno)-1,3,4-Thiadiazole (Fabt) Dmso Solvates. *CrystEngComm* **2013**, *15*, 1978−1988.
(49) Kamiński, D. M.; Hoser, A. A.; Gagoś, M.; Matwijczuk, A.; Arczewska, M.; Niewiadomy, A.; Woźniak, K. Solvatomorphism of 2-(4-Fluorophenylamino)-5-(2,4-Dihydroxybenzeno)-1,3,4-Thiadiazole Chloride. *Cryst. Growth Des.* **2010**, *10*, 3480−3488.
(50) Parkash, J.; Robblee, J. H.; Agnew, J.; Gibbs, E.; Collings, P.; Pasternack, R. F.; de Paula, J. C. Depolarized Resonance Light Scattering by Porphyrin and Chlorophyll a Aggregates. *Biophys. J.* **1998**, *74*, 2089−99.
(51) Binder, H.; Gutberlet, T.; Anikin, A.; Klose, G. Hydration of the Dienic Lipid Dioctadecadienoylphosphatidylcholine in the Lamellar Phase−an Infrared Linear Dichroism and X-Ray Study on Headgroup Orientation, Water Ordering, and Bilayer Dimensions. *Biophys. J.* **1998**, *74*, 1908−1923.
(52) Choosakoonkriang, S.; Wiethoff, C. M.; Koe, G. S.; Koe, J. G.; Anchordoquy, T. J.; Middaugh, C. R. An Infrared Spectroscopic Study of the Effect of Hydration on Cationic Lipid/DNA Complexes. *J. Pharm. Sci.* **2003**, *92*, 115−30.
(53) Korstanje, L. J.; Van Faassen, E. E.; Levine, Y. K. Slow-Motion Esr Study of Order and Dynamics in Oriented Lipid Multibilayers: Effects of Unsaturation and Hydration. *Biochim. Biophys. Acta, Biomembr.* **1989**, *980*, 225−33.
(54) Vlieg, E. Integrated Intensities Using a Six-Circle Surface X-Ray Diffractometer. *J. Appl. Crystallogr.* **1997**, *30*, 532−543.
(55) Dahiya, P.; Kumbhakar, M.; Mukherjee, T.; Pal, H. Effect of Protic Solvents on Twisted Intramolecular Charge Transfer State Formation in Coumarin-152 and Coumarin-481 Dyes. *Chem. Phys. Lett.* **2005**, *414*, 148−154.
(56) Xiaoming, J.; Ziqin, W. Braggs Law with Refractive Correction of Low-Angle X-Ray Diffraction for Periodic Multilayers. *Chin. Phys. Lett.* **1991**, *8*, 356−359.
(57) Kjær, K.; Als-Nielsen, J.; Lahav, M.; Leiserowitz, L.; Kjær, K.; Als-Nielsen, J.; Lahav, M.; Leiserowitz, L. Two-Dimensional Crystallography of Amphiphilic Molecules at the Air-Water Interface. In *Neutron and Synchrotron Radiation for Condensed Matter Studies. Vol. 3. Applications to Soft Condensed Matter and Biology*; Schlenker, C., Schlenker, C., Eds.; Springer-Verlag: Berlin, 1994; pp 47−68.
(58) Wiener, M. C.; Suter, R. M.; Nagle, J. F. Structure of the Fully Hydrated Gel Phase of Dipalmitoylphosphatidylcholine. *Biophys. J.* **1989**, *55*, 315−25.
(59) Kasha, M. Energy Transfer Mechanisms and the Molecular Exciton Model for Molecular Aggregates. *Radiat. Res.* **1963**, *20*, 55−71.
(60) Kasha, M.; Rawls, H. R.; Ashraf El-Bayoumi, M. The Exciton Model in Molecular Spectroscopy. *Pure Appl. Chem.* **1965**, *11*, 371−392.
(61) Graceffa, P.; Lehrer, S. S. The Excimer Fluorescence of Pyrene-Labeled Tropomyosin. A Probe of Conformational Dynamics. *Biochemistry* **1980**, *255*, 11296−11300.

DOI: 10.1021/acs.jpca.5b06475
J. Phys. Chem. A XXXX, XXX, XXX−XXX